At01 Atomic Spectroscopy & Electron Spin Resonance

Matthew Evans

5th December 2018

These experiments investigated the energy transitions involved with electron transitions within the hydrogen atom and energy differences associated with electron spin state changes. The value of the Rydberg constant determined from the atomic spectroscopy experiment was 13.1 ± 0.2 eV and the one given from theory is 13.6 eV [1]. The spectroscopic splitting factor obtained from investigating electron spin resonance was 1.9733 ± 0.0119 and the one given from theory is 2.0023 [2]. These both the experimental values were fairly close to the ones given from theory; however, both of the theoretical values were outside the uncertainty range of the experimental ones. By studying the values of these key atomic constants, many interesting and fundamental concepts, such analysing emission spectra from stars and quantum mechanical properties of atoms, can be investigated in much more detail.

1 Introduction

Two key atomic concepts were investigated during this experiment: the atomic spectrum of hydrogen and the spin resonance of electrons. These two experiments are closely linked and are of key importance when studying atomic characteristics involving the electron. By studying the electron spin we can find that some energy levels of atoms obtained from spectroscopic techniques are further split into smaller energy levels called *multiplets* [3]. From this other phenomena can be more accurately investigated, such as investigating the chemical composition of stars.

Electrons occupy energy levels in atoms that orbit around the nucleus. When electrons gain energy, for example from a collision with an external electron or absorption of a quantum 'packet' of energy called a *photon*, they move up to the next energy level and are then said to be *excited*. After a period of time, they de-excite back to their original energy level emitting a photon equivalent to the energy difference of the two levels

$$h\nu = E_f - E_i \tag{1}$$

where $h = 6.63 \times 10^{-34}$ Js, is the Planck constant, ν is the photon frequency, E_f is the excited energy level, E_i is the original equilibrium energy level. These photon energies can act as 'finger prints' for atoms and hence the particular type of atomic species can be identified by analysing the emitted or absorption spectrum of an atom. Where the absorption spectrum will have particular wavelengths of light missing from a continuous spectrum due to the absorption of photons by the atom from the excitation process. In this experiment we will be analysing the *emitted* spectrum of hydrogen [1].

In addition, all electrons have a spin angular momentum associated with them [2]. The electron spin component is given by

$$S_z = m_s \hbar \tag{2}$$

where S_z is the electron spin angular momentum by considering the z-component, $m_s = \pm\frac{1}{2}$ refers to the spin quantum number either 'spin up' (positive) or 'spin down' (negative) respectively and $\hbar = \frac{h}{2\pi}$. This concept can be likened to an anaology of a spinning sphere [3] where the spin angular momentum is the momentum associated with the body about z-axis. The magnitude of the spin angular momentum is

$$S = \hbar\sqrt{s(s+1)} \tag{3}$$

where $s = \mid m_s \mid = \frac{1}{2}$ and is the spin quantum number. Because electrons have a charge associated with them, they will be affected as they pass through a magnetic field. This experiment investigates this effect further and obtains some fundamental information from this process.

2 Theory

The energy levels of a simplified diagram for the hydrogen atom is shown in Figure 1.

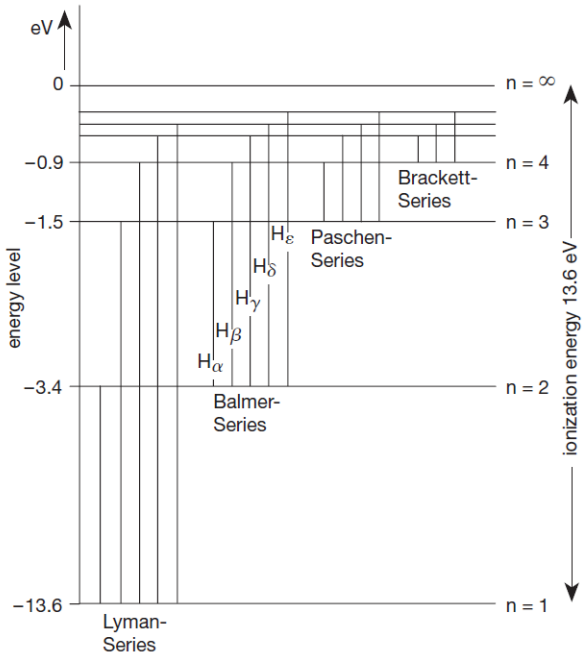

Figure 1: A simplified diagram showing the energy levels of the hydrogen atom. Where n is the principle quantum number. n = 1 is the ground state and n = ∞ correspons to the ionisation energy required to liberate the bound electron [1].

These energy levels can be determined by using the Bohr model or by solution to the Schrödinger equation [1] and is given by

$$E_n = -\frac{Ry}{n^2} \tag{4}$$

where Ry is the Rydberg constant and has a value of 13.6 eV [1] and n is the energy level number in the atom. The experiment considered transitions to the $n = 2$ energy level, i.e. the Balmer Series, for the photon energies as the first few photons in the Balmer Series lie in the visible region of light. This because the first first few energy transitions for this series is in the visible region and can easily be observed. The transitions occur by exposing the the spectral tube to an electric field and this ionises the gas releasing electrons [1]. These free electrons then collide with other electrons bound by hydrogen atoms, as mentioned in Section 1. This excites the bound electrons in the atoms to an excited state. Then, these electrons would de-excite via the emission of a photon, producing a constant output beam. Therefore by considering the relation (1), equation (4) becomes

$$E_n = -Ry\left(\frac{1}{n^2} - \frac{1}{2^2}\right) = Ry\left(\frac{1}{2^2} - \frac{1}{n^2}\right) \tag{5}$$

For a more detailed derivation of the energie levels for the hydrogen atom by solving the Schrödinger equation please refer to [4].

Electrons are negatively charged particles, therefore they have an associated magnetic moment

$$\boldsymbol{\mu} = -g\frac{e}{2m_e}\mathbf{S} \tag{6}$$

μ is the magnetic moment, g is the spectroscopic splitting factor and has a value of 2.0023 for free electrons [2], e is the elemntary charge amd m_e is the rest mass of an electron. As mentioned in Section 1 the spinning motion of the electron is effected as it passes through a magnetic field $\mathbf{B}$ because the magnetic dipoles of the electron and field interact with

each other. This means that the electron will precess about the magnetic field, **B**, in one of two orientations as shown in Figure 2 [2].

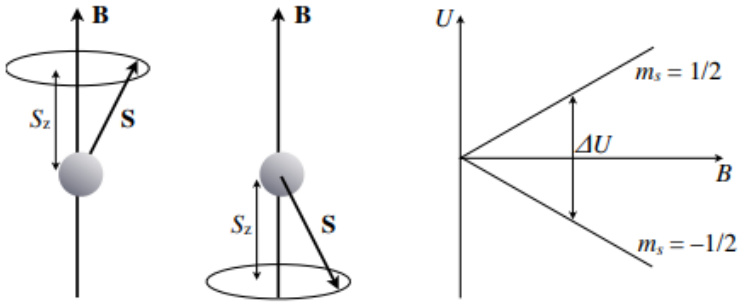

Figure 2: Left: orientation of electron 'spin up' and 'spin down' are given in a magnetic field **B**. Right: dependence of the two energy states on **B** is shown [2].

The magnetic energy is given by [2]

$$U = -\boldsymbol{\mu} \cdot \mathbf{B} = -\mu_z B \tag{7}$$

Where μ_z is the z-component, $\mu_z = -g\frac{e}{2m_e}S_z$, of the magnetic moment. By substituting (2) into (7), we now have

$$U = g\frac{e}{2m_e}(m_s\hbar)B = g\mu_B B \tag{8}$$

where $\mu_B = \frac{e\hbar}{2m_e}$ is the Bohr magneton. Therefore, from Figure 2 and (8) we can see that the difference in energy be determined by [2]

$$\Delta U = g\mu_B B\Big(\frac{1}{2} - \Big(-\frac{1}{2}\Big)\Big) = g\mu_B B. \tag{9}$$

For further information regarding this derivation arriving it equation (9), please refer to [3]. By considering the electron energy changes involved with the atomic spectroscopy mentioned earlier, we can therefore deduce that the electron can either go up or down an energy state by photon absorption or emission receptively. Hence the energy of the photon required for such a transition is given by

$$h\nu = g\mu_B B \tag{10}$$

where ν is again the frequency of the absorbed or emitted photon.

3 Method

3.1 Atomic Spectroscopy

The exerimental set-up is shown in Figure 3.

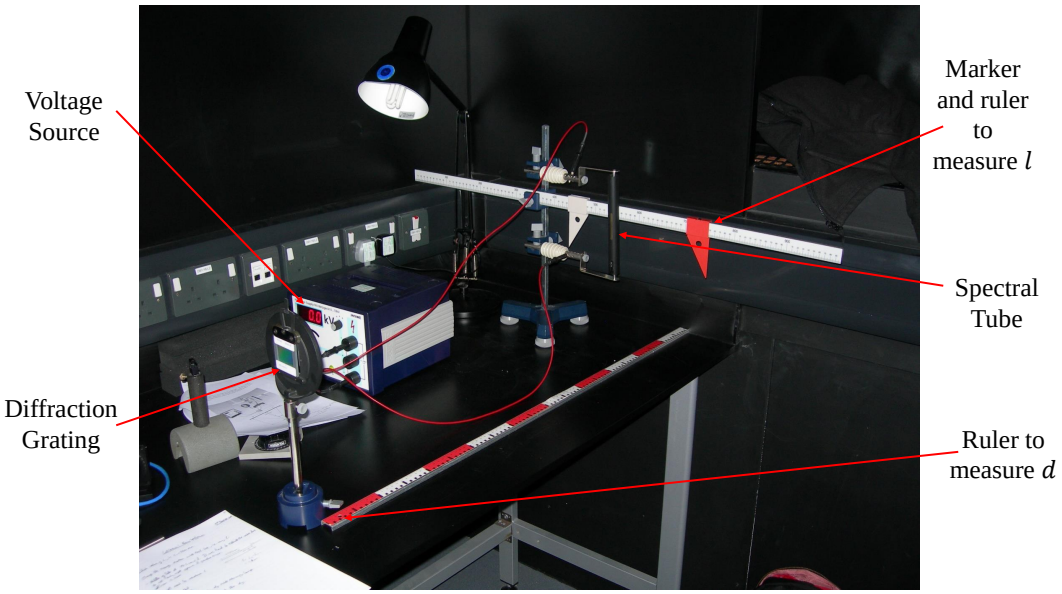

Figure 3: Experimental set-up for the atomic spectroscopy experiment.

First the Hydrogen spectral tube, marker and ruler used to determine l were carefully set-up. The tube was positioned in the centre of the ruler and the measurement taken along with the uncertainty. Then, the diffraction grating was positioned to make the distance from the spectral tube, d, as big as possible. This was carefully measured, along with the associated uncertainty. The low pressure hydrogen gas in the tube was then exposed to an electric field by carefully adjusting the voltage source as shown in Figure 3 so that the spectral tube produced as constant output beam ready for observation. These emission lines were then observed through a diffraction grating as shown in Figure 4 and the marker shown in Figure 3 was adjusted so that the spectral line position could be measured.

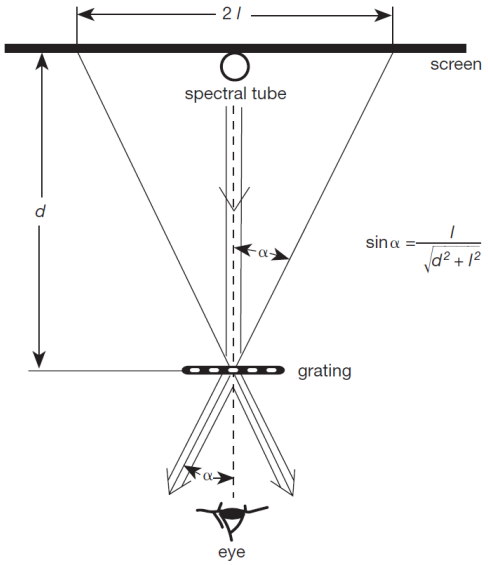

Figure 4: A plan view of the experimental set-up [1].

The difference between the central position of the tube and measured position was then determined along with the associated uncertainties in order to get a value for l. The diffraction grating was then moved in 50mm decrements towards the tube until the lines spectral lines were unclear to view. After this had been undertaken, the diffraction grating was moved back to its original value of d and the above process was then undertaken a total three times to improve accuracy and reduce errors.

The next step was then to use the marker, as shown in Figure 3, to measure the length l of mercury emission lines along the ruler using the mercury lamp in place of the spectral tube in Figure 4 to determine the grating spacing constant d_g. This process was similar to measuring the hydrogen emission lines as outlined above. These measurements were performed for the three furthest distances of d as these were the most accurate. This was repeated a total of three times to reduce uncertainty and improve accuracy. An average of these obtained values of d_g was taken along with its unceratinty carefully determined. Then, by using the known wavelengths of mercury given in [1] and the diffraction grating equation

$$m\lambda = d_g sin\alpha \implies \lambda = d_g \frac{l}{\sqrt{l^2 + d^2}} \tag{11}$$

we can rearrange to determine d_g the grating constant and since we were observing the first bright fringe order, $m = 1$ in this case. The obtained value of d_g, $1.69 \pm 0.02 \times 10^{-6}$m was then compared against the known value 1.67×10^{-6}m [1] and this shows that this is correct with the known value lying within its associated error. Therefore, this check verified that the obtained value of d_g could be used for further calculations. Next, by using the obtained values of l and d an appropriate graph was plotted of l vs $\sqrt{d^2 + l^2}$. The gradient of this graph, $\frac{\lambda}{d_g}$ and the gradient error was used in conjunction with the determined value of d_g and its associated error to determine the wavelength, λ of the sample and error respectively for each of the bright fringes observed.

Once the wavelengths were determined, the energies can were obtained from the relation

$$E = \frac{hc}{\lambda} \tag{12}$$

where, c is the speed of light and λ is the wavelength of the emission lines. Then a graph can be plot using (5) to determine a value for the Rydberg constant Ry.

3.2 Electron Spin Resonance

The sample tested was an organic compound called DPPH (1, 1-diphenyl-2-picrylhydrazil) molecule [2]. The experimental geometry is shown in Figure 5.

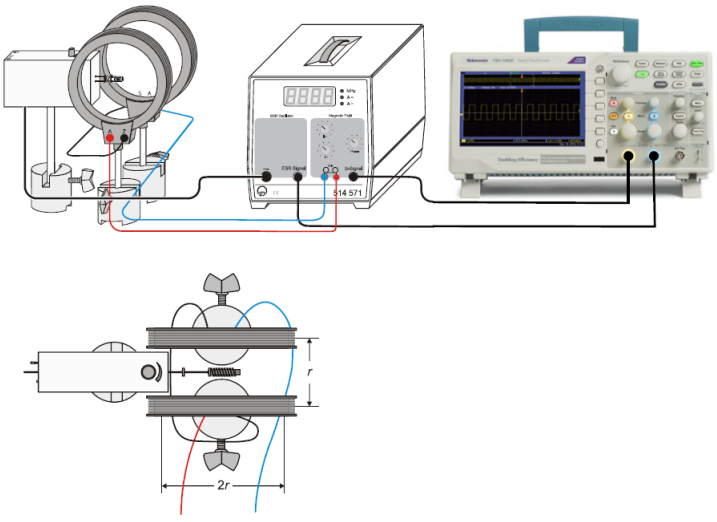

Figure 5: The experimental geometry for investigating electron spin resonance of DPPH [2].

A series of preliminary experiments were conducted before the main experiment. First, the magnetic field produced by the Helmholtz pair of coils were be measured over a range of DC currents using a Gauss meter. A relation describing the magnetic field for this set-up in Figure 5 is given by

$$B = \mu_0 \left(\frac{4}{5}\right)^{3/2} \frac{nI}{r} \tag{13}$$

where μ_0 is the permeability of free space, n is the number of turns per coil ($n = 320$ in this case), I is the current through each coil and r is the distance between the two coils in this case it is the coil radius (6.75cm) [2]. However, the actual distance was greater than this and $r = 7.5 \pm 0.7$cm in this case, due to the width of the radio frequency oscillator having to fit between the two coils to acquire the desired experimental set-up as shown in Figure 7. More will be mentioned about this discrepancy in Section 5. Once a range of magnetic field measurements had been obtained in conjunction with the corresponding currents, these currents were used in (13) to obtain the magnetic field. When comparing the values of the magnetic field measured using the Gauss meter to the ones obtained by relation (13), they were of the same order of magnitude. Therefore, this verified that (13) is a valid way of determining the magnetic field from a range of currents and the next steps in the experimental method could proceed.

The final preliminary check was to see that removing energy from a circuit will put load on the circuit and reduce the output voltage [2].

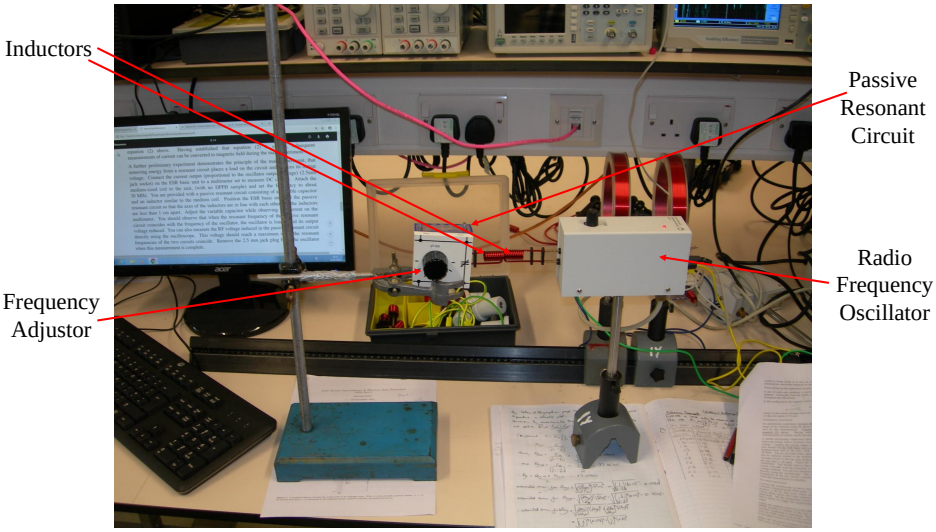

Figure 6: Preliminary Experimental set-up demonstrating a reduction in output voltage due to a load put on a circuit.

The current output from the ESR unit, see Figure 6 was be connected to a multimeter to measure the DC current. Then a passive circuit with a medium inductor coil was positioned close to a medium inductor coil attached to the basic ESR unit, see Figure 6. By adjusting the frequency of the passive circuit, the current reading on the multimeter dropped. This therefore demonstrated that by removing energy from a resonant circuit placed a load on the circuit and the output voltage was reduced. After this principle was checked, the main experiment commenced.

Upon successful completion of the preliminary checks, the DPPH sample was placed in one of the three coils provided and the experiment was set-up in the configuration as shown in Figure 7.

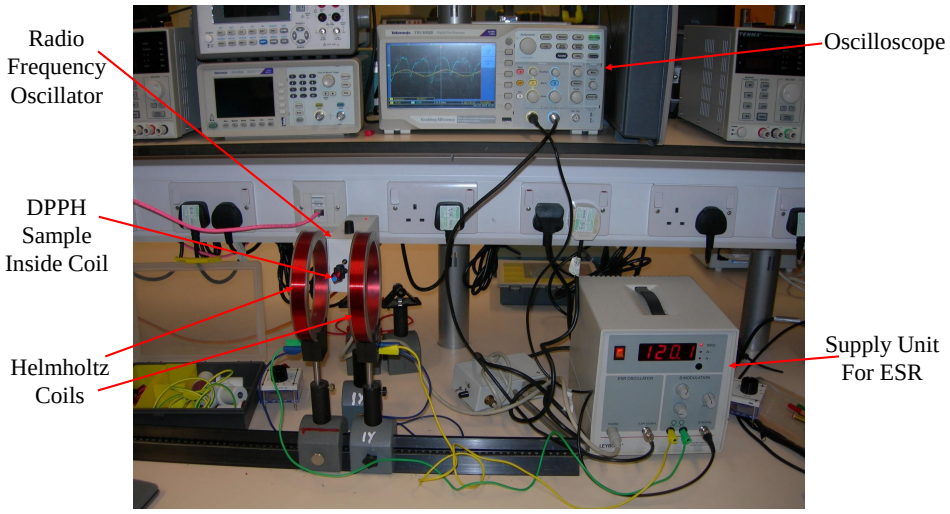

Figure 7: The experimental set-up for investigating the electron spin resonance of DPPH.

Once all the relevant connections had been made to the oscilloscope and the ESR unit, the frequency was altered on the supplit unit for ESR over a range of frequencies from 15 to 130 MHz [2] at different resonances as shown in Figure 8. The range of frequencies were covered by using a selection of sizes for the coils to insert the DPPH sample: small, medium and large.

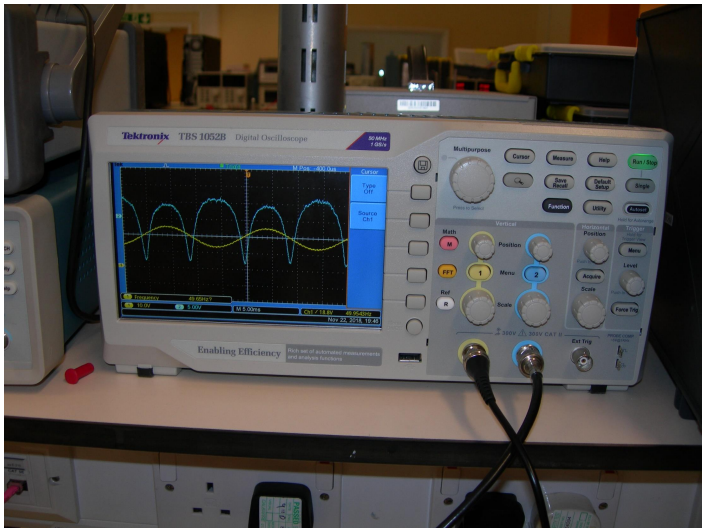

Figure 8: A picture showing the resonant frequency condition as shown on the oscilloscope trace.

Along with these resonant frequencies, the current and corresponding error in the current, obtained from the modulating current, were measured at different resonances from the radio frequency oscillator unit. These resonances were due to a radio frequency photon coming in and exiting an electron from one spin state to another. This takes energy out of the system and is observed as dips on the oscilloscope trace at resonance as shown in Figure 8. Once several resonance measurements for the current had been obtained, using the small, medium and large coils they were all repeated a total of three times and an average current, with corresponding error was taken. This was done to improve accuracy and reliability. Then equation (13) was used to obtain the corresponding magnetic fields. These magnetic field measurements along with the corresponding frequency measurements were used in equation (10) to obtain a value

for g by plotting an appropriate straight-line graph.

3.3 Safety

During both experiments there were many sensitive electrical components used; such as a radio frequency oscillator, an oscolliscope and power supplies. Therefore, no food or drink were consumed whilst working in the laboratory and any exposed metal should was not to be touched when any power supply is switched on [1]. In addition to this, the glass discharge tubes for the Atomic Spectroscopy experiment are fragile. So, when they required moving or changing the demonstrator or laboratory technician were present to handle these pieces of equipment.

4 Results

4.1 Atomic Spectroscopy

Figure 9 and Figure 10 show a plot of l against $\sqrt{d^2+l^2}$ for the two observed hydrogen transitions from the Balmer series: the Hydrogen α, H_α, and Hydrogen β, H_β, transitions.

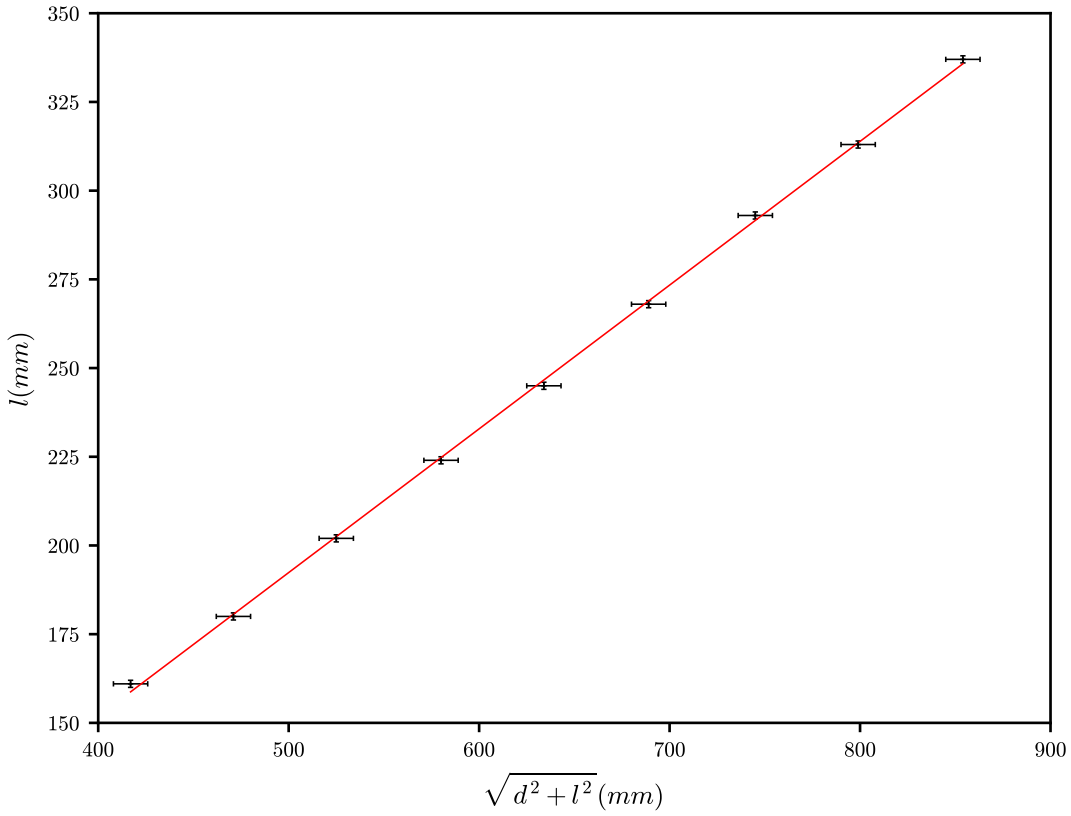

Figure 9: A graph of length l against $\sqrt{d^2+l^2}$ for the H_α transition.

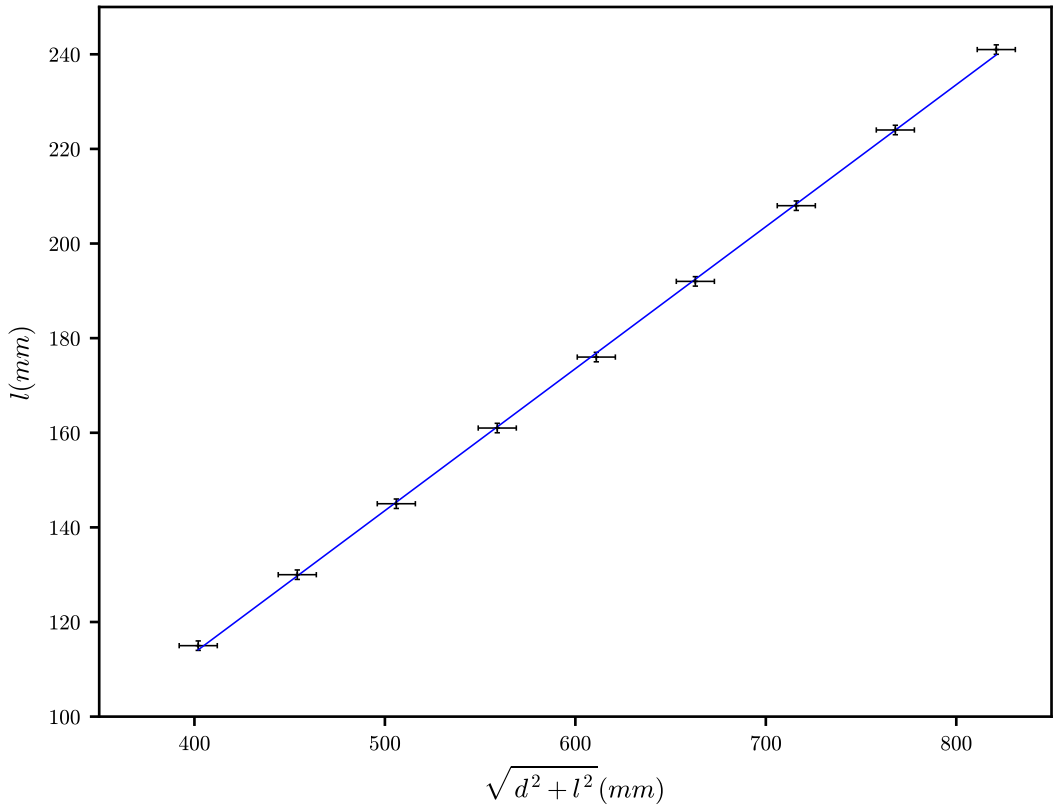

Figure 10: A graph of length l against $\sqrt{d^2+l^2}$ for the H_β transition.

By determining the gradient from Figure 9 and Figure 10 equation (11) was used in the form

$$\lambda = \sigma d_g \tag{14}$$

where $\sigma = \frac{l^2}{\sqrt{l^2+d^2}}$ is the value of the gradient. This equation was used to determine the wavelength for the H_α and H_β transitions. The associated errors for the wavelengths were determined by using

$$\delta\lambda = \sqrt{\left(\frac{\partial\lambda}{\partial\sigma}\right)^2(\delta\sigma)^2 + \left(\frac{\partial\lambda}{\partial d_g}\right)^2(\delta d_g)^2} \tag{15}$$

where $\delta\lambda$ is the error in the wavelength (for H_α or H_β), $\delta\sigma$ is the error in the gradient and δd_g is the error for the determined grating constant. The error for the grating constant was obtained by the usual propagation of errors routine when determining the values of l and d to obtain d_g as mentioned in Section 3.1. Table 1 shows the determined wavelengths from Figure 9 and Figure 10 compared to the theoretical values obtained by performing calculations using equations (5) and (12) and using information from [1].

Table 1: Table of Experimental Values and Theoretical Values for the Transition Wavelengths.

Value	H_α Wavelength, λ_α(nm)	H_β Wavelength, λ_β(nm)
Experimental	685 ± 13	507 ± 8
Theoretical [1]	658	488

Once the wavelengths had been determined, equation (12) was used to find the energy emitted from these transitions.

The associated uncertainty in the energy was then obtained by using the value $\delta\lambda$ in similar propagation methods used for determining the wavelength uncertainty.

Once having obtained the two energies associated with the two transitions, two values of the Rydberg constant could then be determined by using (5) along with their uncertainties by using the uncertainty in the energy of the transitions. These two values were then averaged to determine the value more accurately

$$Ry = \frac{Ry_\alpha + Ry_\beta}{2} \tag{16}$$

where Ry_α and Ry_β are the two values of the Rydberg constant determined from the H_α and H_β transitions respectively. The final uncertainty for the Rydberg constant, δRy, was then determined by

$$\delta Ry = \sqrt{\left(\frac{\partial Ry}{\partial Ry_\alpha}\right)^2 (\delta Ry_\alpha)^2 + \left(\frac{\partial Ry}{\partial Ry_\beta}\right)^2 (\delta Ry_\beta)^2} \tag{17}$$

where δRy_α and δRy_β are the uncertainties for the two values of the Rydberg constant, Ry_α and Ry_β respectively. Table 2 shows a caparison between the experimental and theoretical results of the Rydberg constant.

Table 2: Table of Calculated Values and Published Values for the Rydberg Constant

Value	Rydberg Constant, Ry(eV)
Experimental	13.1 ± 0.2
Theoretical [1]	13.6

4.2 Electron Spin Resonance

Figure 11 shows the results from the determined magnetic fields at various currents from using (13) plotted against different frequencies. This shows a direct linear relation between magnetic field and frequency; showing that an increase in frequency causes the magnetic field to increase as a result.

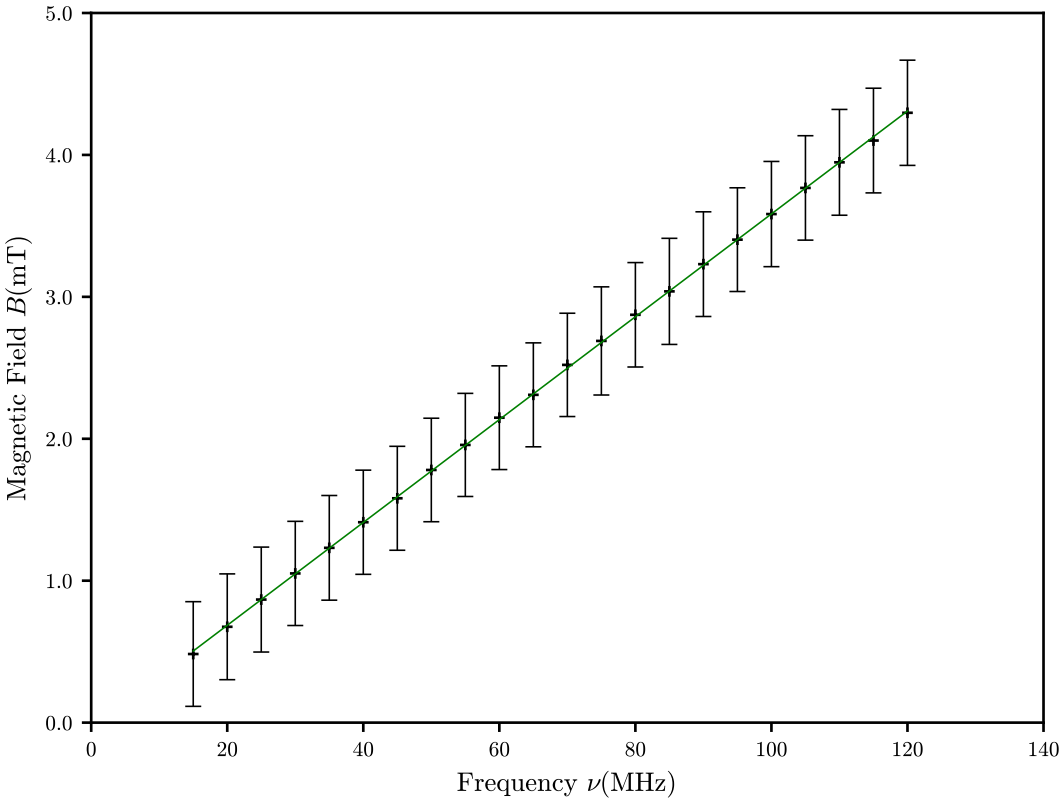

Figure 11: A graph of magnetic field, B against frequency ν.

With reference to Figure 11 equation (10) rearranges to the form of a straight-line graph

$$B = \frac{h}{g\mu_B}\nu = \gamma\nu \tag{18}$$

where $\gamma = \frac{h}{g\mu_B}$ is the gradient of Figure 11. Thus, by obtaining the gradient of the graph and the gradient error, the value of g can be determined. The associated uncertainty of g can be obtained by using

$$\delta g = \sqrt{\left(\frac{\partial g}{\partial \gamma}\right)^2 (\delta\gamma)^2} \tag{19}$$

where δg is the uncertainty in g and $\delta\gamma$ is the error in the gradient of Figure 11. Table 3 compares the values for g determined experimentally to a theoretical value given by [2].

Table 3: Table of Calculated Values and Published Values for the Spectroscopic Splitting Factor.

Value	Spectroscopic Splitting Factor, g
Experimental	1.9733 ± 0.0119
Theoretical [2]	2.0023

5 Discussion

Comparing the results in Section 4.1 Table 2 it is clear to see that the experimental value for the Rydberg constant is close to the theoretical [1]. However, the theoretical value does not lie within the small uncertainty range of the experimental. Also Table 1 shows that the experimental values for the wavelengths are slightly different to those given in theory and again the theoretical values do not lie within the uncertainties of the experimental ones. So, these obtained wavelengths clearly impacted on the final result when obtaining the experimental value of the Rydberg constant and the small uncertainties found from the wavelengths then propagated through to give a small final uncertainty for the Rydberg constant.

We can find the source of these small uncertainty values by inspecting Figure 9 and Figure 10. The error bars in these figures demonstrate that the uncertainties obtained from the experiment are small. When conducting the experiment, many of the uncertainties, such as the ones in the length l and distance d were had to estimate. But from analysis to Figure 9 and Figure 10, the vertical error bars are the smallest. This, therefore suggesting that more consideration should have been taken when estimating the uncertainty in the length, l, of the emission lines across the ruler as described in Section 3.1.

In addition to this, when conducting the atomic spectroscopy experiment, many factors were hard to measure. For example, the emission lines could only be seen in a dark room. But, in this dark environment the length, l, across the ruler was hard to observe due to the dark back ground. Also, some of the emission lines were hard to view at certain distances. Some of the emission lines were faint at large distances, whilst at close distances the angle between d and l was large and this made viewing the emission lines difficult as described in Figure 4. Furthermore, the distance, d, of the diffraction grating from the ruler was also difficult to determine. This was because many factors, such as parallax, made it hard to obtain a result for this value; hence Figure 9 and Figure 10 both show bigger horizontal error bars due to the bigger error in d to accommodate for this discrepancy. All of these values would have impacted on the wavelength values in Table 1 due to using equation (11) to obtain the wavelengths. Hence, the obtained wavelength and associated error would have led to the discrepancies and small error in the experimental value of the Rydberg constant as shown Table 1.

By considering Table 3 we can see that the value of the spectroscopic splitting factor, g, obtained experimentally different to the one given in theory [2]. Also, the theoretical value does not lie within the uncertainty range of the the experimental therefore showing some discrepancies within the experiment. By looking at Figure 11 we can see that the linear fitting line, obtained by the least squares routine, is very accurate and passes through most of the points. This therefore led to a small error in the gradient of the line, $\delta\gamma$ and when propagated through using equation (19) the gave a small error in g. This again, therefore implies that errors within the experiment were small. A possible reason for these small errors is due to the experiment being repeated many times. This reduced the overall error (within the current) and improved confidence when obtaining the values of the current, and hence the magnetic field. Therefore, the error in the result on g was reduced.

Further inspection reveals that the actual experimental value of g is slightly different to what was predicted in theory. When conducting the experiment, numerous factors were hard to determine. For example, the resonance condition was hard to measure. It was hard to get the period of resonance exactly right due to the difficulty in stabilising the frequency from the supply unit. Also, when the resonance conditions were displayed on the oscilloscope, it was hard to deduce exact values of current as there were discrepancies in viewing the period on the grid lines of the screen as shown in Figure 8. By repeating the experiment three times, this reduced some of the inaccuracies within the measurements, but also showed that there was variation within the measured current. This then gave rise to some variation in the magnetic field as shown in the vertical error bars in Figure 11.

In addition to viewing the resonance conditions, when setting up the circuit, the distance between the Helmholtz coils was slightly different to that of the radius of a coil, as mentioned in Section 3.2. This was because the radio frequency oscillator had to fit between the two coils in order to ensure that the DPPH was central in position as shown in Figure 7. Therefore, the actual measured value of r for use in (13) was now 7.5 ± 0.7cm. The large error was used to ensure that had the value of 6.75cm in the range and to accommodate parallax error when setting up the coils. This was all noted and used in equation (13) when determining generated the magnetic fields. Therefore, this would have impacted on the values of g. If more time had been permitted, in order to have obtained a more accurate value of g a different relation would have needed to have been derived for the magnetic field using the Biot-Savhart law. This would have taken into account the different distance between the two Helmholtz coils and hence would have generated a more reliable value of g.

6 Conclusion

Overall, the experiments gave some fairly good values for the Rydberg constant, Ry and spectroscopic splitting factor g. Both of the experiments demonstrate some interesting properties associated with electron energy changes. The atomic spectroscopy experiment demonstrated how electrons change energy levels within the hydrogen atom and the electron spin resonance experiment showed how electrons change spin when exposed to a magnetic field. By taking into account careful estimation of errors and experimental set-ups the experimental results obtained in Section 4.1 Table 2 and Section 4.2 Table 3 would have been more reliable. This would have then showed a stronger correlation between the experimental values and those predicted in theory. However, it is clear to see that these values obtained for Ry and g from the experiments show strong correlations to those given in theory. This verifies that these physical constants are indeed valid when considering atomic and subatomic physics.

References

[1] Atomic Spectroscopy worksheet.

[2] Electron Spin Resonance worksheet.

[3] Young, Hugh D and Freedman, Roger A, *University Physics*, 13^{th} Edition, Chapter 41, pages 1519 - 1527.

[4] Rae, Alastair I.M and Napolitano, Jim, *Quantum Mechanics*, 6^{th} Edition, Chapter 6, pages 115 - 129.